I. J. Mathematical Sciences and Computing, **2025, 2, 10-27**
Published Online on June 8, 2025 by MECS Press (http://www.mecs-press.org/)
DOI: 10.5815/ijmsc.2025.02.02

Mathematical Model of an Infectious Respiratory Disease with a Double-Dose Vaccine, Isolation and Use of Face-Mask

Henry M. Wanjala*
Department of Physical Sciences, Chuka University, Chuka, 60400, Kenya
E-mail: milhenry61@gmail.com
ORCID iD: https://orcid.org/0009-0006-5229-1956
*Corresponding Author

Mark O. Okongo
Department of Physical Sciences, Chuka University, Chuka, 60400, Kenya
E-mail: marikokngo@gmail.com
ORCID iD: https://orcid.org/0000-0002-4198-9594

Jimrise O. Ochwach
Department of Computing Information Technology, Mama Ngina University College, 01030, Kenya
E-mail: ojimrise09@gmail.com
ORCID iD: https://orcid.org/0000-0002-6354-8706

Received: 06 February, 2025; Revised: 22 March, 2025; Accepted: 20 April, 2025; Published: 08 June, 2025

Abstract: Mathematical modeling plays a crucial role in epidemiology by helping us understand how an epidemic unfolds under different conditions. Respiratory infectious diseases have emerged in our history, the virus has significantly impacted all aspects of life. In the absence of a definitive treatment, vaccination and Non-Pharmaceutical Interventions (NPIs) such as social distancing, handwashing, wearing face masks, quarantine, isolation, and contact tracing have been essential in controlling its spread. This study develops a deterministic mathematical model to explore the dynamics of respiratory infectious diseases under key mitigation measures, including vaccination, face mask usage, quarantine, and isolation. The system of Ordinary Differential Equations (ODEs) is solved using Wolfram Mathematica, while the Next Generation Matrix (NGM) method is employed to determine the basic reproduction number. Stability analysis is conducted using the Jacobian matrix, and numerical simulations are carried out in Python using *Jupyter* Notebook. The analysis indicates that the model has a disease-free equilibrium (DFE), which is locally asymptotically stable when the basic reproduction number is less than one. This suggests that respiratory infectious diseases can be effectively controlled if vaccination and NPIs are implemented together. Sensitivity analysis highlights that the most critical factors for eradicating respiratory infectious diseases are the vaccine coverage rate (the proportion of susceptible individuals vaccinated) and vaccine efficacy.

Index Terms: Double-dose vaccination, Face-Mask, Quarantine, Isolation, Stability Analysis, Sensitivity Analysis

1. Introduction

Respiratory pandemics have had profound impacts on both individuals and societies, making it necessary to carefully manage asymptomatic and mildly symptomatic cases within the limits of healthcare resources and facilities [1]. More recently, COVID-19, a novel coronavirus, was first detected in Wuhan, China, in December 2019. By January 2020, the World Health Organization (WHO) officially classified it as a global health threat [2]. This virus marks the third pandemic caused by a novel β-coronavirus since 2002, following the emergence of Severe Acute Respiratory Syndrome Coronavirus (SARS-CoV) in 2002 and Middle East Respiratory Syndrome Coronavirus (MERS-CoV) in 2012 [3, 4, 5]. From the beginning of the outbreak until August 2023, COVID-19 has resulted in over 769 million confirmed cases and more than 6.9 million deaths worldwide. In Kenya alone, there have been 343,955 reported cases and 5,689 deaths, according to WHO data [6].

Governments worldwide have implemented various restrictions and strategies to curb the virus's spread. Alongside these measures, vaccination programs have been rolled out, though their effectiveness varies across different regions.

Mathematical epidemiology has become an essential tool for public health officials, providing insights into disease dynamics and identifying key factors influencing transmission [7, 8]. By using mathematical models, researchers can predict disease patterns, evaluate intervention strategies, and recommend policies to mitigate outbreaks [9]. These models follow established principles of disease transmission and help forecast the impact of control measures [10].

Initially, COVID-19 prevention efforts focused on Non-Pharmaceutical Interventions (NPIs), such as handwashing, social distancing, contact tracing, lockdowns, face mask usage, restrictions on gatherings, isolation, and quarantine. Studies have explored the effectiveness of different face masks in various settings. For instance, research by [11] found that medical face masks are most effective in enclosed environments when used by infected individuals, while cloth masks offer some protection in open community settings. Similarly, [12] highlighted the importance of widespread face mask adoption, showing that both coverage and efficacy play a crucial role in reducing transmission.

Pharmaceutical interventions, including treatment and vaccination, have also played a critical role in controlling COVID-19. Vaccines are designed to trigger an immune response similar to natural infection, reducing the likelihood of severe illness and hospitalization. [13] categorized vaccines into three types: leaky vaccines, all-or-nothing vaccines, and waning vaccines. Studies by [14, 15] further emphasized that vaccination lowers infection risks and reduces the need for intensive medical care.

Researchers have developed various models to study the impact of vaccines alongside NPIs. For example, [16] examined the effect of single-dose vaccines, concluding that high-efficacy vaccines can prolong but moderate an epidemic. Other studies, such as those by [17, 18], explored the role of second-dose vaccines, demonstrating that mass vaccination with a high-efficacy two-dose vaccine, combined with moderate enforcement of NPIs, could help eliminate COVID-19.

Many studies have analyzed the role of NPIs in mitigating COVID-19 transmission, with some focusing on asymptomatic carriers and others on vaccination as a control strategy. However, further research is needed to understand the combined impact of NPIs and vaccination in managing the epidemic, particularly in communities with both symptomatic and asymptomatic individuals.

This study aims to assess how NPIs and vaccination influence COVID-19 transmission in such a population. The paper is structured as follows: Section 2 presents the mathematical model formulation, Section 3 covers the model's mathematical analysis, Section 4 deals with bifurcation analysis, Section 5 presents the sensitivity analysis, Section 6 discusses numerical simulations and results, and Section 7 provides conclusions.

2. Model Formulation

The model is constructed by dividing the total human population at a given time t, represented as $N(t)$, into nine distinct and non-overlapping compartments. These compartments include: susceptible individuals (S), those who have received the first dose of the vaccine (V_1), those who have received the second dose (V_2), exposed individuals (E), those in quarantine (Q), asymptomatic carriers (I_A), symptomatic individuals (I_S), isolated individuals (J), and those who have recovered (R). This classification ensures that every individual in the population belongs to only one of these groups at any given time.

The total human population is given as (1)

$$N(t) = S(t) + V_1(t) + V_2(t) + E(t) + I_A(t) + +I_S(t) + J(t) + R(t) \tag{1}$$

It is assumed that vaccinated individuals still have a probability of getting infected at rates of $(1-\theta_1)$ and $(1-\theta_2)$, where θ_1 and θ_2 denote the efficacy of the first and second vaccine doses, respectively. The susceptible population grows at a rate Λ while individuals across all compartments experience a natural death rate μ.

The vaccination rates for the first and second doses are represented by α_1 and α_2, respectively. A proportion of the susceptible individuals become exposed due to a force of infection λ. Contact tracing leads to a fraction q of exposed individuals being quarantined, while a fraction n transitions into the asymptomatic class after a latency period of ω. The remaining $(1-n)$ fraction of exposed individuals develop symptoms after the latency period.

Following the quarantine period z, confirmed cases are either isolated at a rate ρ or return to the susceptible pool. It is assumed that individuals in the asymptomatic class are unaware of their COVID-19 status and, therefore, do not take precautionary measures.

Individuals in the exposed, isolated, and symptomatic compartments experience a reduction in infectivity by factors ϵ_1, ϵ_2, ϵ_3, respectively. All symptomatic individuals are isolated at a rate γ. Isolated individuals recover at a rate ρ_I or succumb to the disease at a rate Φ_J, while symptomatic individuals die at a rate Φ_S. Asymptomatic individuals recover at a rate ρ_1.

A fraction c_m of the public adheres to public health guidelines on wearing face masks correctly, with an efficacy level denoted by ϵ_m. The effective contact rate is represented by β.

The model flow chart is shown in Fig. 1:

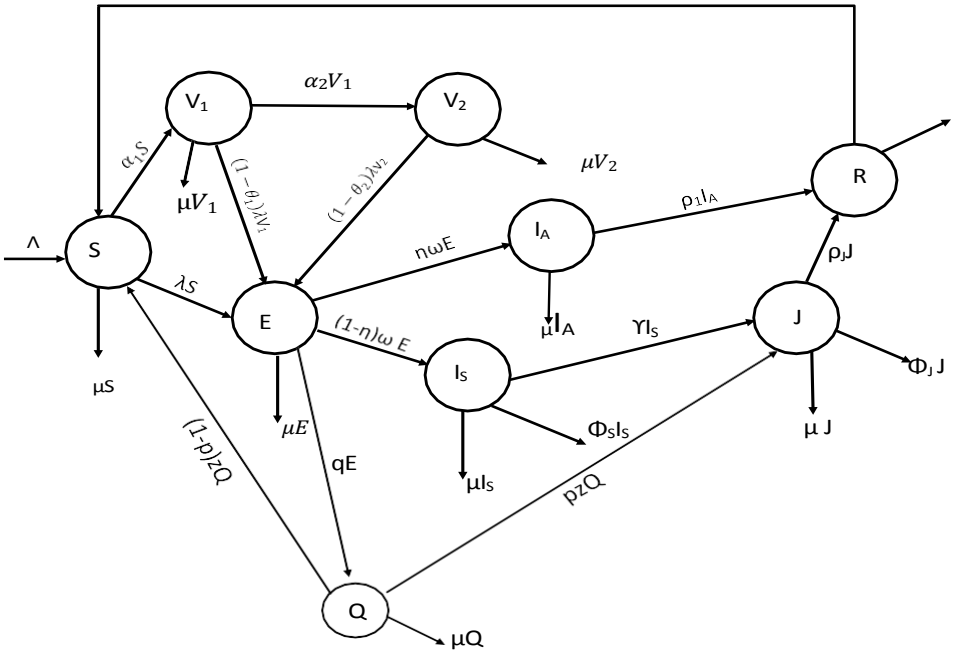

Fig. 1. Model Flow Chart 1

Based on the schematic diagram in Fig. 1., the corresponding system of differential equations is derived and presented in (2)

$$\frac{dS}{dt} = \Lambda + \delta R + (1-p)zQ - (\alpha_1 + \lambda + \mu)S \tag{2}$$

$$\frac{dV_1}{dt} = \alpha_1 S - (\mu + \alpha_2 + (1-\theta_1)\lambda)V_1$$

$$\frac{dV_2}{dt} = \alpha_2 V_1 - (\mu + (1-\theta_2)\lambda)V_2$$

$$\frac{dE}{dt} = \lambda S + (1-\theta_1)\lambda V_1 + (1-\theta_2)\lambda V_2 - (\mu + \omega + q)E$$

$$\frac{dQ}{dt} = qE - (\mu + z)Q$$

$$\frac{dI_A}{dt} = \eta\omega E - (\mu + \rho_1)I_A$$

$$\frac{dI_S}{dt} = (1-\eta)\omega E - (\mu + \phi_s + \gamma)I_S$$

$$\frac{dJ}{dt} = \gamma I_S + pzQ - \left(\mu + \phi_J + \rho_J\right)$$

$$\frac{dR}{dt} = \rho_1 I_A + \rho_J J - (\mu + \delta)R$$

The equation that describes the force of infection, denoted as λ, is (3). The modification parameters ϵ_m and c_m account for the impact of mask-wearing on disease transmission, where ϵ_m represents the efficacy of masks in reducing infection risk, and c_m reflects the consistency and compliance of individuals in wearing masks properly. A higher ϵm $\epsilon_m c_m$ value indicates greater reduction in transmission. The infectious contributors in the force of infection equation include different compartments of infected individuals: I_A (asymptomatic infectious), I_S (symptomatic infectious), J (hospitalized cases), and E (exposed individuals who may contribute to transmission before symptoms appear). Each category has a corresponding parameter (ϵ_3, ϵ_2, ϵ_1) to scale its infectiousness relative to asymptomatic cases, adjusting for factors like increased viral shedding or reduced contact rates in hospitalized individuals.

$$\lambda = \beta\big((1-\epsilon_m c_m)(I_A + \epsilon_3 I_S + \epsilon_2 J + \epsilon_1 E)\big)/N \tag{3}$$

The Table 1. shows the model parameters.

Table 1. Parameter Values 1

Symbol	Parameter	Value	Source
Λ	Recruitment rate by birth	0.00018 $days^{-1}$	[19]
μ	Natural death rate	4.563×10^{-5} $days^{-1}$	[25]
ϕ	Disease induced mortality	0.0018	[19]
α_1	initial dose vaccine administration rate	8.157×10^{-7}	[18]
α_2	second dose vaccine administration rate	0.974	[18]
θ_1	Vaccine efficacy of first dose	Assumed at 0.8	[25]
θ_2	Vaccine efficacy of second dose	Assumed at 0.95	[25]
p	Fraction of those isolated after quarantine	0.8	Assumed
ρ_1	Rate of recovery of asymptomatic patients	0.97	[20]
ρ_J	Rate of recovery of isolated patients	0.0714	[19]
ω	Latency period	0.03	Assumed
Γ	rate of isolation of symptomatic patients	0.04	Assumed
Δ	Waning rate of immunity	0.06	Assumed
β	Effective contact rate	0.5 $days^{-1}$	[21]
z	Quarantine period	1/14 days	[22]
cm	Proportion of the population that consistently and accurately wears face masks	0.1	[14]
ϵm	Efficacy of face mask	0.5	[14].
ϵ_1	Infections by the Exposed	0.48	[21]
ϵ_2	infections by the Isolated	0.48	[21]
ϵ_3	Infections y the symptomatics	0.48	[21]
η	Fraction of those Asymptomatic but Infectious	0.7	[19]
Q	Rate of transfer of E to Q	2.0138×10^{-4}	[22]

In this study, we assume specific vaccine coverage rates to illustrate their impact on disease transmission. These rates are based on hypothetical scenarios to demonstrate potential outcomes under different vaccination strategies. However, in real-world settings, vaccine coverage is influenced by factors such as availability, public acceptance, logistical constraints, and government policies. Future studies could incorporate data-driven approaches or sensitivity analyses to explore the variability and determinants of vaccine coverage.

3. Model Analysis

In this section, basic reproduction number, stability analysis of disease-free and endemic equilibrium point is discussed.

3.1. Basic Reproduction Number

The basic reproduction equation and its corresponding number quantify the transmission potential of an infectious disease. It represents the average number of secondary infections generated by a single infected individual introduced into a fully susceptible population. This equation is derived using the next generation matrix (NGM). To determine the reproduction number, the Jacobian matrix obtained from the model equations is analyzed.

Theorem 1. *The basic reproductive equation (R_o) for the epidemiological model 2 is expressed in (4).*

$$\mathcal{R}_0 = \frac{m\beta_0\epsilon_1}{k_1} + \frac{m\beta_0\eta\omega}{k_1k_3} + \frac{m\beta_0\epsilon_3(1-\eta)\omega}{k_1k_4} + \frac{m\beta_0\epsilon_2\gamma(1-\eta)\omega k_2 - pzk_4}{k_1k_2k_4k_5} \tag{4}$$

where:

$$m = \Lambda\left(\frac{\mu^2 + [\alpha_2 + (1-\theta_1)\alpha_1]\mu + (1-\theta_2)\alpha_2\alpha_1}{\mu(\mu+\alpha_1)(\mu+\alpha_2)}\right)$$

And

$$k_1 = \mu + \omega + q, \qquad k_2 = \mu + z,\ k_3 = \mu + \rho_1, \qquad k_4 = \mu + \phi_S, \qquad k_5 = \mu + \phi_J + \rho_J, \qquad \beta_0 = \beta(1 - \epsilon_m c_m)$$

According to [26], the infectious subsystem is deduced from (2) as shown in (5):

$$\frac{dE}{dt} = \lambda S + (1-\theta_1)\lambda V_1 + (1-\theta_2)\lambda V_2 - (\mu+\omega+q)E$$
$$\frac{dQ}{dt} = qE - (\mu+z)Q$$
$$\frac{dI_A}{dt} = \eta\omega E - (\mu+\rho_1)I_A$$
$$\frac{dI_S}{dt} = (1-\eta)\omega E - (\mu+\phi_s+\gamma)I_S$$
$$\frac{dJ}{dt} = \gamma I_S + pzQ - (\mu+\phi_J+\rho_J)J \quad (5)$$

The Jacobian matrix is decomposed into two matrices in (6) and (7)

$$F=\begin{pmatrix} m\beta_0\epsilon_1 & 0 & m\beta_0 & m\beta_0\epsilon_3 & m\beta_0\epsilon_2 \\ 0 & 0 & 0 & 0 & 0 \\ 0 & 0 & 0 & 0 & 0 \\ 0 & 0 & 0 & 0 & 0 \\ 0 & 0 & 0 & 0 & 0 \end{pmatrix} \quad (6)$$

$$V = \begin{pmatrix} -k_1 & 0 & m\beta_0 & m\beta_0\epsilon_3 & m\beta_0\epsilon_2 \\ 0 & -k_2 & 0 & 0 & 0 \\ \eta\omega & 0 & -k_3 & 0 & 0 \\ (1-\eta)\omega & 0 & 0 & -k_4 & 0 \\ 0 & pz & 0 & \mu & -k_5 \end{pmatrix} \quad (7)$$

Where,

$$k_1 = \mu+\omega+q, \quad k_2 = \mu+z, \quad k_3 = \mu+\rho_1,$$
$$k_4 = \mu+\phi_s+\gamma, \quad k_5 = \mu+\phi_j+\rho_J, \quad \beta_0 = \beta(1-\epsilon_m c_m)$$

By computing V^{-1} yields equation (8)

$$V^{-1} = \begin{pmatrix} \frac{-1}{k_1} & 0 & 0 & 0 & 0 \\ \frac{-q}{k_1k_2} & \frac{-1}{k_2} & 0 & 0 & 0 \\ \frac{-\eta\omega}{k_1k_3} & 0 & \frac{-1}{k_3} & 0 & 0 \\ \frac{-(1-\eta)\omega}{k_1k_4} & 0 & 0 & \frac{-1}{k_4} & 0 \\ \frac{-\gamma(1-\eta)\omega k_2 - pzk_4}{k_1k_2k_4k_5} & \frac{-pz}{k_5k_2} & 0 & \frac{-\gamma}{k_4k_5} & \frac{-1}{k_5} \end{pmatrix} \quad (8)$$

Therefore, the basic reproduction number for the system model (2) is calculated by finding the spectral radius of the matrix FV^{-1}, as shown in (9).

$$FV^{-1} = \begin{pmatrix} a & \frac{\beta_0\epsilon_1 pz}{k_2k_5} & \frac{\beta_0}{k_3} & \frac{m\beta_0\epsilon_1}{k_4} + \frac{\beta_0\epsilon_3\gamma}{k_4k_5} & \frac{m\beta_0\epsilon_2}{k_5} \\ 0 & 0 & 0 & 0 & 0 \\ 0 & 0 & 0 & 0 & 0 \\ 0 & 0 & 0 & 0 & 0 \\ 0 & 0 & 0 & 0 & 0 \end{pmatrix} \quad (9)$$

Where, $a = \frac{m\beta_0\epsilon_1}{k_1} + \frac{m\beta_0\eta\omega}{k_1k_3} + \frac{m\beta_0\epsilon_3(1-\eta)\omega}{k_1k_4} + \frac{m\beta_0\epsilon_2\gamma(1-\eta)\omega k_2 - pzk_4}{k_1k_2k_4k_5}$

Thus, the basic reproduction number is given in (10):

$$\mathcal{R}_0 = \frac{m\beta_0\epsilon_1}{k_1} + \frac{m\beta_0\eta\omega}{k_1k_3} + \frac{m\beta_0\epsilon_3(1-\eta)\omega}{k_1k_4} + \frac{m\beta_0\epsilon_2\gamma(1-\eta)\omega k_2 - pzk_4}{k_1k_2k_4k_5} \quad (10)$$

3.2. Local Stability Analysis of Disease-Free Equilibrium

Assume the first order partial derivatives of f and g are continuous in some open set containing the equilibrium point (x^*, y^*). Then, the equilibrium is locally asymptotically stable if:

1. Tr (J) < 0, and
2. det (J) > 0 where, J is the Jacobian matrix evaluated at the equilibrium. In addition, the equilibrium is unstable if either Tr(J) > 0 or Det(J) < 0.

The local stability analysis is performed by constructing the Jacobian matrix of the model system (2) and solving it at the DFE yielding (11):

$$\mathcal{J}_f = \begin{pmatrix} k_1 & 0 & 0 & \varepsilon_1 M & (1-p)z & -M & \varepsilon_3 M & \varepsilon_2 M & \delta \\ \alpha_1 & k_2 & 0 & \varepsilon_1 Z & 0 & Z & \varepsilon_3 Z & \varepsilon_2 Z & 0 \\ 0 & \alpha_2 & k_3 & \varepsilon_1 P & 0 & P & \varepsilon_3 P & \varepsilon_2 P & 0 \\ 0 & 0 & 0 & E_1 + k_4 & 0 & I_{A1} & I_{S1} & J_1 & 0 \\ 0 & 0 & 0 & q & k_5 & 0 & 0 & 0 & 0 \\ 0 & 0 & 0 & \eta\omega & 0 & k_6 & 0 & 0 & 0 \\ 0 & 0 & 0 & (1-\eta)\omega & 0 & 0 & k_7 & 0 & 0 \\ 0 & 0 & 0 & 0 & pz & 0 & \gamma & k_8 & 0 \\ 0 & 0 & 0 & 0 & 0 & \rho_1 & 0 & \rho_J & k_9 \end{pmatrix} \quad (11)$$

Where,

$$k_1 = -(\alpha_1 + \mu), k_2 = -(\mu + \alpha_2), k_3 = -(\mu), k_4 = -(\mu + \omega + q) + \beta\epsilon_1 S, k_5 = -(\mu + z), k_6 = -(\mu + \rho_1), k_7 = -(\mu + \phi_s + \gamma), k_8 = -(\mu + \phi_J + \rho_J), k_9 = -(\mu + \delta), M = \beta(1 - \epsilon_m c_m)\left(\frac{\mu(\mu+\alpha_2)}{\mu^2+(\mu+2\alpha_1)\alpha_2}\right), Z = \beta(1 - \epsilon_m c_m)(1 - \theta_1)\left(\frac{\mu\alpha_1}{\mu^2+(\mu+2\alpha_1)\alpha_2}\right), p = \beta(1 - \epsilon_m c_m)(1 - \theta_2)\left(\frac{\alpha_2\alpha_1}{\mu^2+(\mu+2\alpha_1)\alpha_2}\right), E_1 = \epsilon_1 M + \epsilon_1 Z + \epsilon_1 P, I_{A_1} = M + Z + P, I_{S_1} = \epsilon_3 M + \epsilon_3 Z + \epsilon_3 P, J_1 = \epsilon_2 M + \epsilon_2 Z + \epsilon_2 P$$

From (11) above and the numerical substitution of the parameters from Table 1, it is determined that:

1. Tr (J_f) = -2.96625 < 0, and,
2. Det (J_f) = 3.11028 > 0

Thus, the DFE is locally asymptotically stable.

3.3. Global Stability Analysis of Disease-Free Equilibrium

Theorem 2. Consider the autonomous system defined by $\hat{x} = f(x)$, with the equilibrium point of interest being the origin. Let A(x) denote the Jacobian matrix of the system, $A(x) = \frac{\partial f}{\partial x}$. If the matrix $F = A + A^T$ is negative neighborhood Ω, then, the equilibrium point at the origin is asymptotically stable. A Lyapunov function for this system is

$$V(x) = f^T(x)f(x) \quad (12)$$

If Ω is the entire state space and, in addition, $V(x) \to \infty$, $[\|x\|] \to \infty$, then, the equilibrium point is said to be globally asymptotically stable.

To conduct the global stability analysis, we create the Jacobian matrix for the model system (2) and evaluate it at the Disease-Free Equilibrium (DFE), as demonstrated in (13):

$$F(x) = \begin{pmatrix} k_1 & 0 & 0 & \varepsilon_1 M & (1-p)z & -M & \varepsilon_3 M & \varepsilon_2 M & \delta \\ \alpha_1 & k_2 & 0 & \varepsilon_1 Z & 0 & Z & \varepsilon_3 Z & \varepsilon_2 Z & 0 \\ 0 & \alpha_2 & k_3 & \varepsilon_1 P & 0 & P & \varepsilon_3 P & \varepsilon_2 P & 0 \\ 0 & 0 & 0 & E_1 + k_4 & 0 & I_{A1} & I_{S1} & J_1 & 0 \\ 0 & 0 & 0 & q & k_5 & 0 & 0 & 0 & 0 \\ 0 & 0 & 0 & \eta\omega & 0 & k_6 & 0 & 0 & 0 \\ 0 & 0 & 0 & (1-\eta)\omega & 0 & 0 & k_7 & 0 & 0 \\ 0 & 0 & 0 & 0 & pz & 0 & \gamma & k_8 & 0 \\ 0 & 0 & 0 & 0 & 0 & \rho_1 & 0 & \rho_J & k_9 \end{pmatrix} \quad (13)$$

where,

$$k_1 = -(\alpha_1 + \mu), k_2 = -(\mu + \alpha_2), k_3 = -(\mu), k_4 = -(\mu + \omega + q) + \beta\epsilon_1 S, k_5 = -(\mu + z), k_6 = -(\mu + \rho_1), k_7 = -(\mu + \phi_s + \gamma), k_8 = -\left(\mu + \phi_J + \rho_J\right), k_9 = -(\mu + \delta), M = \beta(1 - \epsilon_m c_m)\left(\frac{\mu(\mu+\alpha_2)}{\mu^2+(\mu+2\alpha_1)\alpha_2}\right), Z = \beta(1 - \epsilon_m c_m)(1 - \theta_1)\left(\frac{\mu\alpha_1}{\mu^2+(\mu+2\alpha_1)\alpha_2}\right), p = \beta(1 - \epsilon_m c_m)(1 - \theta_2)\left(\frac{\alpha_2\alpha_1}{\mu^2+(\mu+2\alpha_1)\alpha_2}\right), E_1 = \epsilon_1 M + \epsilon_1 Z + P, \quad I_{A_1} = M + Z + P, I_{S_1} = \epsilon_3 M + \epsilon_3 Z + \epsilon_3 P, J_1 = \epsilon_2 M + \epsilon_2 Z + \epsilon_2 P$$

From (13) above, the transpose ($F^T(x)$) of F(x) is as shown in (14):

$$\mathrm{F^T\ (X)} = \begin{pmatrix} k_1 & \alpha_1 & 0 & 0 & 0 & 0 & 0 & 0 & 0 \\ 0 & k_2 & \alpha_2 & 0 & 0 & 0 & 0 & 0 & 0 \\ 0 & 0 & k_3 & 0 & 0 & 0 & 0 & 0 & 0 \\ -\varepsilon_1 M & -\varepsilon_1 Z & -\varepsilon_1 P & E_1 + k_4 & q & \eta\omega & (1-\eta)\omega & 0 & 0 \\ (1-p)z & 0 & 0 & q & k_5 & 0 & 0 & pz & 0 \\ -M & Z & P & I_{A1} & 0 & k_6 & 0 & 0 & \rho_1 \\ -\varepsilon_3 M & -\varepsilon_3 Z & -\varepsilon_3 P & I_{S1} & 0 & 0 & k_7 & 0 & 0 \\ -\varepsilon_2 M & -\varepsilon_2 Z & -\varepsilon_2 P & J_1 & 0 & 0 & \gamma & k_8 & \rho_J \\ \delta & 0 & 0 & 0 & 0 & 0 & 0 & 0 & k_9 \end{pmatrix} \tag{14}$$

From the matrix above, $\hat{\mathrm{F}}(\mathrm{x})$ is as shown in (15):

$$\hat{F}(x) = F^T(x) + F(x) \tag{15}$$

This implies that $\hat{\mathrm{F}}(\mathrm{x}))$ is as in (16):

$$\hat{\mathrm{F}}(\mathrm{x}) = \begin{pmatrix} 2k_1 & \alpha_1 & 0 & -\varepsilon_1 M & (1-p)z & -M & -\varepsilon_3 M & -\varepsilon_2 M & \delta \\ 0 & 2k_2 & \alpha_2 & -\varepsilon_1 Z & 0 & -Z & -\varepsilon_3 Z & -\varepsilon_2 Z & 0 \\ 0 & 0 & 2k_3 & 0 & 0 & -P & -\varepsilon_3 P & -\varepsilon_2 P & 0 \\ -\varepsilon_1 M & -\varepsilon_1 Z & -\varepsilon_1 P & A & q & \mathrm{D} & E & J_1 & 0 \\ (1-p)z & 0 & 0 & q & 2k_5 & 0 & 0 & pz & 0 \\ -M & Z & P & B & 0 & 2k_6 & 0 & 0 & \rho_1 \\ -\varepsilon_3 M & -\varepsilon_3 Z & -\varepsilon_3 P & C & 0 & 0 & 2k_7 & 0 & 0 \\ -\varepsilon_2 M & -\varepsilon_2 Z & -\varepsilon_2 P & J_1 & pz & 0 & \gamma & 2k_8 & \rho_J \\ \delta & 0 & 0 & 0 & 0 & 0 & 0 & 0 & 2k_9 \end{pmatrix} \tag{16}$$

$$A = 2k_4 + 2E_1, B = \eta\omega + I_{A_1}, k_1 = -(\alpha_1 + \mu), C = (1-\eta)\omega + I_{S_1}, k_2 = -(\mu + \alpha_2), D = \eta\omega + I_{A_1}, E = (1-\eta)\omega + I_{S_1}, k_3 = -(\mu), k_4 = -(\mu + \omega + q) + \beta\epsilon_1 S, k_5 = -(\mu + z), k_6 = -(\mu + \rho_1), k_7 = -(\mu + \phi_s + \gamma), k_8 = -\left(\mu + \phi_J + \rho_J\right), k_9 = -(\mu + \delta), M = \beta(1 - \epsilon_m c_m)\left(\frac{\mu(\mu+\alpha_2)}{\mu^2+(\mu+2\alpha_1)\alpha_2}\right), Z = \beta(1 - \epsilon_m c_m)(1 - \theta_1)\left(\frac{\mu\alpha_1}{\mu^2+(\mu+2\alpha_1)\alpha_2}\right), P = \beta(1 - \epsilon_m c_m)(1 - \theta_2)\left(\frac{\alpha_2\alpha_1}{\mu^2+(\mu+2\alpha_1)\alpha_2}\right), E_1 = \epsilon_1 M + \epsilon_1 Z + \epsilon_1 P, I_{A_1} = M + Z + P, I_{S_1} = \epsilon_3 M + \epsilon_3 Z + \epsilon_3 P, J_1 = \epsilon_2 M + \epsilon_2 Z + \epsilon_2 P$$

If A is a negative definite matrix of order n, then Tr(A) < 0. If n is even, Det(A) > 0 and if n is odd, Det(A) < 0. Since both conditions are satisfied, then, the matrix is negative definite.

So, the matrix $F^T(x)$ is negative definite. This, is a Lyapunov function for the system F(x), and thus,

$$V(x) = f^T(x)f(x) \tag{17}$$

and, in addition, $V(x) \to \infty$, $[||x||] \to \infty$, then, the equilibrium point is said to be globally asymptotically stable.

3.4. Local Stability Analysis of Endemic Equilibrium

Computing the Jacobian matrix at the Equilibrium Point (EE) of (2) results in (18):

$$\mathcal{J}_f = \begin{pmatrix} k_1 & 0 & 0 & \varepsilon_1 M & (1-p)z & -M & \varepsilon_3 M & \varepsilon_2 M & \delta \\ \alpha_1 & k_2 & 0 & \varepsilon_1 Z & 0 & Z & \varepsilon_3 Z & \varepsilon_2 Z & 0 \\ 0 & \alpha_2 & k_3 & \varepsilon_1 P & 0 & P & \varepsilon_3 P & \varepsilon_2 P & 0 \\ \lambda^* & (1-\theta_1)\lambda^* & (1-\theta_2)\lambda^* & E_1 + k_4 & 0 & I_{A1} & I_{S1} & J_1 & 0 \\ 0 & 0 & 0 & q & k_5 & 0 & 0 & 0 & 0 \\ 0 & 0 & 0 & \eta\omega & 0 & k_6 & 0 & 0 & 0 \\ 0 & 0 & 0 & (1-\eta)\omega & 0 & 0 & k_7 & 0 & 0 \\ 0 & 0 & 0 & 0 & pz & 0 & \gamma & k_8 & 0 \\ 0 & 0 & 0 & 0 & 0 & \rho_1 & 0 & \rho_J & k_9 \end{pmatrix} \quad (18)$$

Where,

$$k_1 = -(\alpha_1 + \mu), k_2 = -(\mu + \alpha_2), k_3 = -(\mu), k_4 = -(\mu + \omega + q) + \beta\epsilon_1 S, k_5 = -(\mu + z), k_6 = -(\mu + \rho_1), k_7 = -(\mu + \phi_s + \gamma), k_8 = -(\mu + \phi_J + \rho_J), k_9 = -(\mu + \delta), M = \beta(1-\epsilon_m c_m)\left(\frac{\mu(\mu+\alpha_2)}{\mu^2+(\mu+2\alpha_1)\alpha_2}\right), Z = \beta(1-\epsilon_m c_m)(1-\theta_1)\left(\frac{\mu\alpha_1}{\mu^2+(\mu+2\alpha_1)\alpha_2}\right), p = \beta(1-\epsilon_m c_m)(1-\theta_2)\left(\frac{\alpha_2\alpha_1}{\mu^2+(\mu+2\alpha_1)\alpha_2}\right), E_1 = \epsilon_1 M + \epsilon_1 Z + \epsilon_1 P, I_{A_1} = M + Z + P, I_{S_1} = \epsilon_3 M + \epsilon_3 Z + \epsilon_3 P, J_1 = \epsilon_2 M + \epsilon_2 Z + \epsilon_2 P, \lambda^* = \beta(1-\epsilon_m c_m)(I_A^* + \epsilon_3 I_S^* + \epsilon_2 J^* + \epsilon_1 E^*)/N$$

From (18) above and the numerical substitution of the parameters in Table 1, it is determined that:

1. Tr (J_f) < 0, and,
2. Det (J_f) > 0

Thus, the EE is locally asymptotically stable.

3.5. Global Stability Analysis of Endemic Equilibrium

The analysis of global stability for the endemic equilibrium is carried out by forming the Jacobian matrix for the model system (2) and solving it at the Equilibrium Point (EE), resulting in (19):

$$\mathrm{F(x)} = \begin{pmatrix} k_1 & 0 & 0 & \varepsilon_1 M & (1-p)z & -M & \varepsilon_3 M & \varepsilon_2 M & \delta \\ \alpha_1 & k_2 & 0 & \varepsilon_1 Z & 0 & Z & \varepsilon_3 Z & \varepsilon_2 Z & 0 \\ 0 & \alpha_2 & k_3 & \varepsilon_1 P & 0 & P & \varepsilon_3 P & \varepsilon_2 P & 0 \\ \lambda^* & (1-\theta_1)\lambda^* & (1-\theta_2)\lambda^* & E_1 + k_4 & 0 & I_{A1} & I_{S1} & J_1 & 0 \\ 0 & 0 & 0 & q & k_5 & 0 & 0 & 0 & 0 \\ 0 & 0 & 0 & \eta\omega & 0 & k_6 & 0 & 0 & 0 \\ 0 & 0 & 0 & (1-\eta)\omega & 0 & 0 & k_7 & 0 & 0 \\ 0 & 0 & 0 & 0 & pz & 0 & \gamma & k_8 & 0 \\ 0 & 0 & 0 & 0 & 0 & \rho_1 & 0 & \rho_J & k_9 \end{pmatrix} \quad (19)$$

Where,

$$k_1 = -(\alpha_1 + \mu), k_2 = -(\mu + \alpha_2), k_3 = -(\mu), k_4 = -(\mu + \omega + q) + \beta\epsilon_1 S, k_5 = -(\mu + z), k_6 = -(\mu + \rho_1), k_7 = -(\mu + \phi_s + \gamma), k_8 = -(\mu + \phi_J + \rho_J), k_9 = -(\mu + \delta), M = \beta(1-\epsilon_m c_m)\left(\frac{\mu(\mu+\alpha_2)}{\mu^2+(\mu+2\alpha_1)\alpha_2}\right), Z = \beta(1-\epsilon_m c_m)(1-\theta_1)\left(\frac{\mu\alpha_1}{\mu^2+(\mu+2\alpha_1)\alpha_2}\right), p = \beta(1-\epsilon_m c_m)(1-\theta_2)\left(\frac{\alpha_2\alpha_1}{\mu^2+(\mu+2\alpha_1)\alpha_2}\right), E_1 = \epsilon_1 M + \epsilon_1 Z + \epsilon_1 P, I_{A_1} = M + Z + P, I_{S_1} = \epsilon_3 M + \epsilon_3 Z + \epsilon_3 P, J_1 = \epsilon_2 M + \epsilon_2 Z + \epsilon_2 P, \lambda^* = \beta(1-\epsilon_m c_m)(I_A^* + \epsilon_3 I_S^* + \epsilon_2 J^* + \epsilon_1 E^*)/$$

From (19) above, the transpose ($F^T(x)$) of F(x) is (20):

$$\mathrm{F^T\,(X)} = \begin{pmatrix} k_1 & \alpha_1 & 0 & \lambda^* & 0 & 0 & 0 & 0 & 0 \\ 0 & k_2 & \alpha_2 & f & 0 & 0 & 0 & 0 & 0 \\ 0 & 0 & k_3 & h & 0 & 0 & 0 & 0 & 0 \\ -\varepsilon_1 M & -\varepsilon_1 Z & -\varepsilon_1 P & j & q & \eta\omega & (1-\eta)\omega & 0 & 0 \\ (1-p)z & 0 & 0 & q & k_5 & 0 & 0 & pz & 0 \\ -M & Z & P & I_{A1} & 0 & k_6 & 0 & 0 & \rho_1 \\ -\varepsilon_3 M & -\varepsilon_3 Z & -\varepsilon_3 P & I_{S1} & 0 & 0 & k_7 & 0 & 0 \\ -\varepsilon_2 M & -\varepsilon_2 Z & -\varepsilon_2 P & J_1 & 0 & 0 & \gamma & k_8 & \rho_J \\ \delta & 0 & 0 & 0 & 0 & 0 & 0 & 0 & k_9 \end{pmatrix} \quad (20)$$

Where,

$$a = k_2 - (1-\theta_1)\lambda, b = (1-\theta_1)\lambda, c = k_3 - (1-\theta_2)\lambda, d = E_1 + k_4, k_1 = -(\alpha_1 + \mu), k_2 = -(\mu + \alpha_2), k_3 = -(\mu), k_4 = -(\mu + \omega + q) + \beta\epsilon_1 S, k_5 = -(\mu + z), k_6 = -(\mu + \rho_1), k_7 = -(\mu + \phi_s + \gamma), k_8 = -\left(\mu + \phi_J + \rho_J\right), k_9 = -(\mu + \delta), M = \beta(1-\epsilon_m c_m)\left(\frac{\mu(\mu+\alpha_2)}{\mu^2 + (\mu + 2\alpha_1)\alpha_2}\right),$$
$$Z = \beta(1-\epsilon_m c_m)(1-\theta_1)\left(\frac{\mu\alpha_1}{\mu^2 + (\mu + 2\alpha_1)\alpha_2}\right), p = \beta(1-\epsilon_m c_m)(1-\theta_2)\left(\frac{\alpha_2\alpha_1}{\mu^2 + (\mu + 2\alpha_1)\alpha_2}\right), E_1 = \epsilon_1 M + \epsilon_1 Z + \epsilon_1 P, I_{A_1} = M + Z + P, \quad I_{S_1} = \epsilon_3 M + \epsilon_3 Z + \epsilon_3 P$$

From (20) above, $\hat{F}(x)$ is now determined by (21):

$$\hat{F}(x) = F^T(x) + F(x) \tag{21}$$

so as to get (22):

$$\hat{F}(x) = \begin{pmatrix} a_1 & \alpha_1 & 0 & a_2 & (1-p)z & -M & -\varepsilon_3 M & -\varepsilon_2 M & \delta \\ 0 & a_3 & \alpha_2 & a_4 & 0 & -Z & -\varepsilon_3 Z & -\varepsilon_2 Z & 0 \\ 0 & \alpha_2 & a_5 & a_6 & 0 & -P & -\varepsilon_3 P & -\varepsilon_2 P & 0 \\ a_7 & a_8 & a_9 & a_{10} & q & \mathrm{D} & E & J_1 & 0 \\ (1-p)z & 0 & 0 & q & 2k_5 & 0 & 0 & pz & 0 \\ -M & Z & P & A & 0 & 2k_6 & 0 & 0 & \rho_1 \\ -\varepsilon_3 M & -\varepsilon_3 Z & -\varepsilon_3 P & B & 0 & 0 & 2k_7 & 0 & 0 \\ -\varepsilon_2 M & -\varepsilon_2 Z & -\varepsilon_2 P & J_1 & pz & 0 & \gamma & 2k_8 & \rho_J \\ \delta & 0 & 0 & 0 & 0 & 0 & 0 & 0 & 2k_9 \end{pmatrix} \tag{22}$$

Where,

$$a_1 = 2k_1 - 2\lambda, a_2 = -\epsilon_1 M - \lambda, a_3 = 2k_2 - 2(1-\theta_1)\lambda, a_4 = -\epsilon_1 Z + (1-\theta_1)\lambda, a_5 = 2k_3 - 2(1-\theta_2)\lambda, a_6 = -\epsilon_1 P + (1-\theta_2)\lambda, a_7 = \lambda - \epsilon_1 M, a_8 = -\epsilon_1 Z + (1-\theta_1)\lambda, a_9 = -\epsilon_1 P + (1-\theta_2)\lambda, a_{10} = 2k_4 + 2E_1, k_1 = -(\alpha_1 + \mu), k_2 = -(\mu + \alpha_2), k_3 = -(\mu), k_4 = -(\mu + \omega + q) + \beta\epsilon_1 S, k_5 = -(\mu + z), k_6 = -(\mu + \rho_1), k_7 = -(\mu + \phi_s + \gamma), k_8 = -\left(\mu + \phi_J + \rho_J\right), k_9 = -(\mu + \delta), M = \beta(1-\epsilon_m c_m)\left(\frac{\mu(\mu+\alpha_2)}{\mu^2 + (\mu + 2\alpha_1)\alpha_2}\right), Z = \beta(1-\epsilon_m c_m)(1-\theta_1)\left(\frac{\mu\alpha_1}{\mu^2 + (\mu + 2\alpha_1)\alpha_2}\right), p = \beta(1-\epsilon_m c_m)(1-\theta_2)\left(\frac{\alpha_2\alpha_1}{\mu^2 + (\mu + 2\alpha_1)\alpha_2}\right)$$

To ascertain the global asymptotic stability of the model system (2) at the endemic equilibrium, we employ the Lyapunov-Krasovskii method.

From the numerical analysis:

1. Tr $(F(x)) < 0$
2. Det $(F(x)) > 0$

Therefore, the matrix, $\hat{F}(x)$ does not exhibit negative definiteness, leading us to the conclusion that the model (2) is globally asymptotically unstable at the endemic equilibrium. Thus, it is necessary to perform a bifurcation analysis to determine if there are sufficient and necessary circumstances under which the epidemic may persist in the community.

4. Bifurcation Analysis

Theorem 3. (As outlined by [25]). Consider the following general system of ordinary differential equations with a parameter ϕ.

$$\frac{dx}{dt} = f(x, 0), f: \mathrm{R}^n \times R \to R \text{ and } \mathrm{f} \in C^2(R^n \times R) \tag{23}$$

Where 0 is an equilibrium point of the system (that is, f $(0, \phi) = 0, \forall\phi$) and assume:

a $A = D_x f(0,0) = \left[\frac{\partial f_i}{\partial x_j}(0,0)\right]$ is the linearization matrix of 21 around the equilibrium point 0 with ϕ evaluated at 0, zero is a simple eigenvalue of A and other eigenvalues of A have negative real parts.

b Matrix A has a right eigenvector w and left eigenvector v (each corresponding to zero eigenvalues)

Let f_k be k −th component of f and

a $a = \sum_{k,i,j=1}^{n} v_k w_i w_j \frac{\partial^2 f_k}{\partial x_i \partial x_j}(0,0)$

b $b = \sum_{k,i=1}^{n} v_k w_i \frac{\partial^2 f_k}{\partial x_i \partial \theta}(0,0)$

The local dynamics of the system (2) around 0 is totally determined by the signs of a and b.

(i) a > 0, b > 0, when $\phi < 0$ with $|\phi| \ll 1$, 0 is locally asymptotically stable and there exists a positive unstable equilibrium; when $0 < \phi \ll 1$, 0 is unstable and there exist a negative and locally asymptotically stable equilibrium.

(ii) a < 0, b < 0. When $\phi < 0$ with $|\phi| \ll 1$, 0 is locally asymptotically stable and there exists a positive unstable equilibrium; when $0 < \phi \ll 1$, 0 is unstable and there exist a positive unstable equilibrium.

(iii) a > 0, b < 0, when $\phi < 0$ with $|\phi| \ll 1$, 0 is unstable, and there exists a locally asymptotically stable negative equilibrium; when $0 < \phi \ll 1$, 0 is stable, and a positive unstable equilibrium appears.

(iv) a < 0, b > 0, When ϕ changes from negative to positive, 0 changes its stability from stable to unstable. Correspondingly a negative unstable equilibrium becomes positive and locally asymptotically stable.

In what follows, let the model system (2) be written in the vector form

$$\frac{dX}{dt} = G(X)$$

Where $X = (x_1, x_2, x_3, x_4, x_5, x_6, x_7, x_8, x_9)^T$ and $G = (g_1, g_2, g_3, g_4, g_5, g_6, g_7, g_8, g_9)$. So that $S = x_1, V_1 = x_2, V_2 = x_3, E = x_4, Q = x_5, I_A = x_6, I_S = x_7, J = x_8, R = x_9$, then the model system (2) yields (24):

$$\begin{aligned}
\frac{dx_1}{dt} &= \Lambda + \delta x_9 + (1-p)zx_5 - (\alpha_1 + \lambda + \mu)x_1 \\
\frac{dx_2}{dt} &= \alpha_1 x_1 - (\mu + \alpha_2 + (1-\theta_1)\lambda)x_2 \\
\frac{dx_3}{dt} &= \alpha_2 x_2 - (\mu + (1-\theta_2)\lambda)x_3 \\
\frac{dx_4}{dt} &= \lambda x_1 + (1-\theta_1)\lambda x_2 + (1-\theta_2)\lambda x_3 - (\mu + \omega + q)x_4 \\
\frac{dx_5}{dt} &= qx_4 - (\mu + z)x_5 \\
\frac{dx_6}{dt} &= \eta\omega x_4 - (\mu + \rho_1)x_6 \\
\frac{dx_7}{dt} &= (1-\eta)\omega x_4 - (\mu + \phi_s + \gamma)x_7 \\
\frac{dx_8}{dt} &= \gamma x_8 + pzx_5 - (\mu + \phi_J + \rho_J)x_8 \\
\frac{dx_9}{dt} &= \rho_1 x_6 + \rho_J x_8 - (\mu + \delta)x_9
\end{aligned} \tag{24}$$

Let β be the bifurcation parameter then at $R_0 = 1$ in (24) and solving for β yields (25):

$$\beta = \hat{\beta} = \frac{k_1 k_2 k_3 k_4 k_5}{m(1-\epsilon_m c_m)\left(pzqk_3k_4\epsilon_2 + k_2\left(k_4k_5(\eta\omega + k_3\epsilon_1) + (1-\eta)\omega k_3(\epsilon_2\gamma + \epsilon_3 k_5)\right)\right)} \tag{25}$$

The disease-free equilibrium, denoted as E_0, exhibits local stability when $\beta < \hat{\beta}$ and instability when β exceeds $\hat{\beta}$. Hence, $\hat{\beta}$ serves as the bifurcation point. The linearized matrix of the system (24), calculated around the disease-free equilibrium E_0 and assessed at $\hat{\beta}$, is presented in equation (26):

$$\mathcal{J}(E_0|\hat{\beta}) = \begin{pmatrix} k_1 & 0 & 0 & a_1 & a_6 & a_8 & a_{12} & a_{16} & \delta \\ \alpha_1 & k_2 & 0 & a_2 & 0 & a_9 & a_{13} & a_{17} & 0 \\ 0 & \alpha_2 & k_3 & a_3 & 0 & a_{10} & a_{14} & a_{18} & 0 \\ 0 & 0 & 0 & k_4 & 0 & a_{11} & a_{15} & a_{19} & 0 \\ 0 & 0 & 0 & q & k_5 & 0 & 0 & 0 & 0 \\ 0 & 0 & 0 & a_4 & 0 & k_6 & 0 & 0 & 0 \\ 0 & 0 & 0 & a_5 & 0 & 0 & k_7 & 0 & 0 \\ 0 & 0 & 0 & 0 & a_7 & 0 & 0 & k_8 & 0 \\ 0 & 0 & 0 & 0 & 0 & \rho_1 & 0 & 0 & k_8 \end{pmatrix} \tag{26}$$

where,

$$\begin{aligned} k_1 = -(\alpha_1 + \mu), k_2 = -(\mu + \alpha_2), k_3 = -(\mu), k_4 = -(\mu + \omega + q) + \beta\epsilon_1 S, k_5 = -(\mu + z), k_6 = -(\mu + \rho_1), k_7 \\ = -(\mu + \phi_s + \gamma), k_8 = -\left(\mu + \phi_J + \rho_J\right), k_9 = -(\mu + \delta), a_1 = -\epsilon_1 S, a_2 = -\epsilon_1(1 - \theta_1)V_1, a_3 \\ = -\epsilon_1(1 - \theta_2)V_2, k_4 = -a_1 - a_2 - a_3, a_4 = \eta\omega, a_5 = (1 - \eta)\omega, a_6 = (1 - p)z, a_7 = pz, a_8 \\ = -S, a_9 = (1 - \theta_1)V_1, a_{10} = -(1 - \theta_1)V_2, a_{11} = -a_8 - a_9 - a_{10}, a_{12} = \epsilon_3 S, a_{13} \\ = -\epsilon_3(1 - \theta_1)V_1, a_{14} = -\epsilon_3(1 - \theta_2)V_2, a_15 = -a_{12} - a_{13} - a_{14}, a_16 = -\epsilon_2 S, 1_{17} \\ = -\epsilon_2(1 - \theta_1)V_1, a_{18} = -\epsilon_3(1 - \theta_2)V_2, a_{19} = -a_{16} - a_{17} - a_{18} \end{aligned}$$

The eigenvalues denoted as (λ_h) of the Jacobian matrix J($E_0|\hat{\beta}$) are solutions to the characteristic equation. These eigenvalues form polynomials of eighth degree, all of which have real roots that are negative, except for one eigenvalue which is zero. It's apparent that zero is a single, simple eigenvalue of the Jacobian matrix J($E_0|\hat{\beta}$), and all the other eigenvalues are equal and negative. Consequently, the disease-free equilibrium E_0 is a non-hyperbolic equilibrium, which aligns with the assumption made in Theorem 3.

Hence, we utilize the center manifold theorem to assess the local stability of the disease-free equilibrium point E_0. The right eigenvector $m = (m_1, m_2, m_3, m_4, m_5, m_6, m_7, m_8, m_9)^T$ and left eigenvector $v = (v_1, v_2, v_3, v_4, v_5, v_6, v_7, v_8, v_9)$ associated with this simple zero eigenvalue of the matrix J($E_0|\hat{\beta}$) such that $v.m = 1$, can be obtained from J($E_0,\hat{\beta}$) by multiplying vJ and mJ and setting each of them equal to zero. The resulting system of the right eigenvalues become (27):

$$\begin{gathered} m_1k_1 + m_4ak_1 + m_5k_6 + m_6a_8 + m_7a_{12} + m_8a + 16 + \delta = 0 \\ m_1\alpha_1 + m_2k_2 + m_4a_2 + m_6a_9m_7a_{13} + m_8a_{17} = 0 \\ m_2\alpha_2 + m_3k_3 + m_4a_3 + m_6a_{10} + m_7a_{14} + m_8a_{18} = 0 \\ m_4k_4 + m_6a_{11} + m_7a15 + m_8a_{19} = 0 \\ m_4q + m_5k_5 = 0 \\ m_4a_4 + m_6k_6 = 0 \\ m_4a_5 + m_7k_7 = 0 \\ m_5a_7 + m_8k_8 = 0 \\ m_6\rho_1 + m_8\rho_J + m_9k_9 = 0 \end{gathered} \tag{27}$$

Let, $m_4 = m_4 > 0$

Then,

$$\begin{aligned} m_1 = -\frac{am_4}{k_1}, m_2 = -\frac{bm_4}{k_2}, m_3 = -\frac{cm_4}{k_3}, m_5 = -\frac{k_5m_4}{q}, m_6 = -\frac{a_4m_4}{k_6}, m_7 = -\frac{a_5m_4}{k_7}, m_8 = \frac{a_7k_5m_4}{qk_8}, m_9 = \frac{m_{10}}{m_4} \\ m_{10} = \frac{m_4}{k_9}\left(\frac{\rho_1a_4}{k_6} - \frac{a_7k_5m_4\rho_J}{qk_8}\right), -a = m_4a_1 - \frac{k_5a_6m_4}{q} - \frac{a_4a_6m_4}{k_6} - \frac{a_5a_{12}m_4}{k_7} + \frac{a_7a_{18}k_5m_4}{qk_8} + m_{10}m_4, b \\ = \frac{\alpha_1m_4}{k_1} + a_3m_4 - \frac{-a_{10}a_4m_4}{k_6} - \frac{a_{14}a_5m_4}{k_7} + \frac{a_7k_5a_{18}m_4}{qk_8}, c \\ = -m_2a_2 - m_4a_3 - m_6a_1 0 - m_7a_{14} + m_8a_{18} \end{aligned}$$

Further, the left eigenvector, $v = (v_1, v_2, v_3, v_4, v_5, v_6, v_7, v_8, v_9)$ corresponding to the simple zero eigenvalue of is obtained from $v\mathcal{J}\left(E_0, \hat{\beta}\right) = 0$, which yields equation (28):

$$\begin{gathered} v_1k_1 + v_2\alpha_1 = 0 \\ v_2k_2 + v_3\alpha_2 = 0 \\ v_3k_3 = 0 \\ v_1a_1 + v_2a_2 + v_3a_3 + v_4k_4 + v_5q + v_6a_4 + v_7a_5 = 0 \\ v_1a_6 + v_5k_5 + v_8a_7 = 0 \\ v_1a_8 + v_2a_9 + v_3a_{10} + v_4a_{11} + v_6k_6 + v_9\rho_1 = 0 \\ v_1a_{12}v_2a_{13} + v_3a_{14} + v_4a_{15} + v_7k_7 = 0 \end{gathered} \tag{28}$$

$$v_1a_{16} + v_2a_{17} + v_3a_{17} + v_3a18 + v_4a_{19} + v_8k_8 + v_9\rho_J = 0$$
$$v_1\delta + v_9k_9 = 0$$

From equation 28 we obtain $v_1 = v_2 = v_3 = v_9 = 0$ and,
let, $v_4 > 0$,
then,

$$v_5 = \frac{a_7a_{19}v_4}{k_5k_8}, v_6 = -\frac{a_{11}v_4}{k_6}, v_7 = -\frac{a_{15}v_4}{k_7}, v_8 = -\frac{a_{19}v_4}{k_8}$$

In order to meet the condition where $v.m = 1$, we calculate the value of v_4. To compute the bifurcation coefficients a and b defined in Theorem 3, we consider system model (2) to be in the form:

$$\frac{dX}{dt} = f = (f_1, f_2, f_3, f_4, f_5, f_6, f_7, f_8, f_9)^T \tag{29}$$

Where $X = (x_1, x_2, x_3, x_4, x_5x_6, x_7, x_8, x_9)^T$.
The coefficient a and b are obtained from the following partial derivatives in (30) and (31) respectively.

$$a = \sum_{k,i,j=1}^{10} v_k m_i m_j \frac{\partial^2 f_k}{\partial x_i \partial x_j}(0,0) \tag{30}$$

And,

$$b = \sum_{k,i=1}^{10} v_k m_i \frac{\partial^2 f_k}{\partial x_i \partial \xi}(0,0) \tag{31}$$

Since the components of v_1,v_2,v_3,v_9 are zero we do not need to find the derivatives of f_1,f_2,f_3,f_9. From the derivative of the remaining f_4,f_5,f_6,f_7,f_8, the only ones that have non-zero partial derivatives are considered such that:

$$\frac{\partial^2 f_4}{\partial x_1 \partial x_4} = \frac{\partial^2 f_4}{\partial x_4 \partial x_1} = \epsilon_1, \frac{\partial^2 f_4}{\partial x_1 \partial x_6} = \frac{\partial^2 f_4}{\partial x_6 \partial x_1} = 1$$
$$\frac{\partial^2 f_4}{\partial x_1 \partial x_7} = \frac{\partial^2 f_4}{\partial x_7 \partial x_1} = \epsilon_3, \frac{\partial^2 f_4}{\partial x_1 \partial x_8} = \frac{\partial^2 f_4}{\partial x_8 \partial x_1} = \epsilon_2$$
$$\frac{\partial^2 f_4}{\partial x_2 \partial x_4} = \frac{\partial^2 f_4}{\partial x_4 \partial x_2} = \left(1_{\theta_1}\right)\epsilon_1, \frac{\partial^2 f_4}{\partial x_2 \partial x_6} = \frac{\partial^2 f_4}{\partial x_6 \partial x_2} = (1-\theta_1)$$
$$\frac{\partial^2 f_4}{\partial x_2 \partial x_7} = \frac{\partial^2 f_4}{\partial x_7 \partial x_2} = (1-\theta_1)\epsilon_3, \frac{\partial^2 f_4}{\partial x_2 \partial x_7} = \frac{\partial^2 f_4}{\partial x_7 \partial x_2} = (1-\theta_1)\epsilon_3$$
$$\frac{\partial^2 f_4}{\partial x_2 \partial x_8} = \frac{\partial^2 f_4}{\partial x_8 \partial x_2} = (1-\theta_1)\epsilon_2, \frac{\partial^2 f_4}{\partial x_3 \partial x_4} = \frac{\partial^2 f_3}{\partial x_4 \partial x_3} = (1-\theta_2)\epsilon_1$$
$$\frac{\partial^2 f_4}{\partial x_3 \partial x_6} = \frac{\partial^2 f_4}{\partial x_6 \partial x_3} = (1-\theta_2), \frac{\partial^2 f_4}{\partial x_3 \partial x_7} = \frac{\partial^2 f_3}{\partial x_7 \partial x_3} = (1-\theta_2)\epsilon_3$$
$$\frac{\partial^2 f_4}{\partial x_3 \partial x_8} = \frac{\partial^2 f_4}{\partial x_8 \partial x_3} = (1-\theta_2)\epsilon_2 \tag{32}$$

The indication of either having a forward or backward bifurcation is determined by a. Consequently, it yields (33):

$$a = 2v_4m_1m_4\epsilon + 2v_4m_1m_6 + 2v_4m_1m_7\epsilon_3 + 2v_4m_1m_8\epsilon_2 + 2v_4m_2m_4(1-\theta_1)\epsilon_1 + 2v_4m_2m_6(1-\theta_1) + 2v_4m_2m_7(1-\theta_1)\epsilon_3 + 2v_4m_2m_8(1-\theta_1)\epsilon_2 + 2v_4m_2m_4(1-\theta_2)\epsilon_1 + 2v_4m_2m_6(1-\theta_2) + 2v_4m_2m_7(1-\theta_2)\epsilon_3 + 2v_4m_2m_8(1-\theta_2)\epsilon_2 > 0 \tag{33}$$

Thus, a system of equations in (2), undergoes a backward bifurcation at $R_\iota = 1$, if $\beta > \hat{\beta}$ (effective contact rate). This implies that, the eradication of COVID - 19 may not be guaranteed by just ensuring that $R_\iota < 0$. There is a possibility that they might be a recurrence of the epidemic later on.

5. Sensitivity Analysis

The normalized forward-sensitivity index of a variable R_o, that depends differentiably on parameter, μ_i is defined as in (34):

$$\Upsilon_{\mu_i}^{\mathcal{R}_c} = \frac{\partial \mathcal{R}_0}{\partial \mu_i} \times \frac{\mu_i}{\mathcal{R}_\sigma} \tag{34}$$

Where μ_i represents all the main parameters and

$$\mathcal{R}_0 = \frac{m\beta_0\epsilon_1}{k_1} + \frac{m\beta_0\eta\omega}{k_1k_3} + \frac{m\beta_0\epsilon_3(1-\eta)\omega}{k_1k_4} + \frac{m\beta_0\epsilon_2\gamma(1-\eta)\omega k_2 - pzk_4}{k_1k_2k_4k_5}$$

Based on the given definition, we can calculate the sensitivity indices of the basic reproduction number R_0 concerning the model parameters within the system model (2), as presented in (34):

To find the sensitivity index of the effect of wearing face-mask, we proceed as shown in (35):

$$\Upsilon_{\mu_1}^{\mathcal{R}_\sigma} = \frac{\partial \mathcal{R}_\sigma}{\partial c_m} \times \frac{c_m}{\mathcal{R}_\sigma}$$
$$= -\frac{c_m\epsilon_m}{1 - c_m\epsilon_m} \leq 0$$

Clearly, $\Upsilon_{\mu_1}^{\mathcal{R}_\sigma} \leq 0$ from observation in (35), then, the sensitivity index of the wearing of face-mask is negative, an increase in this factor results in a reduction in the control reproduction number, which subsequently leads to a reduction in transmission. Thus, to reduce transmission of SARS-COV-2 there's a need to enforce wearing of face-masks. To find the sensitivity index of the impact of the efficacy of a given face mask (ϵ_m) it is proceeded as shown in (36):

$$\Upsilon_{\xi}^{\mathcal{R}_\sigma} = \frac{\partial \mathcal{R}_\sigma}{\partial \epsilon_m} \times \frac{\epsilon_m}{\mathcal{R}_\sigma}$$
$$= -\frac{c_m\epsilon_m}{1 - c_m\epsilon_m} \leq 0$$

Since the sensitivity index of ϵ_m is negative, an increase in the efficacy of the face - mask leads to a decrease in the control reproduction number, leading to a decrease in transmission. Thus, to reduce transmission of SARS-COV-2 there's a need to use a face - mask with a higher efficacy. Similar procedure can be used to calculate the sensitivity indices of other parameters around the basic reproduction number which is summarized in Table 2.

Table 2. Sign of Sensitivity Index 1

Parameter	SI
η	Positive
ω	Positive
ϕ_S	Negative
ϕ_J	Negative
ρ_1	Negative
ρ_J	Negative
γ	Negative
z	Negative
α_1	Negative
α_2	Negative
p	Negative

In order to determine the most efficient method for reducing the spread of COVID-19, we evaluated the importance of each parameter in impacting its transmission. Based on the numerical application of parameter values, it is essential to ascertain the function of each parameter in relation to the basic reproduction number. Through numerical analysis, it becomes evident that the effective contact rate (β) is the parameter with the most pronounced influence in elevating the basic reproduction number, followed by an increase in the fraction of asymptomatic cases. It is also established that, an increase in the vaccine coverage rate of the first dose vaccine (α_1) will lower the basic reproduction number the greatest.

6. Numerical Analysis

The ordinary differential equations used to obtain the numerical solutions were implemented in Python and solved using the *numpy* and *scipy* solvers. This study focuses on Kenya, with some parameter values being specific to the country while others remain universal. To facilitate comparison and analysis, certain parameters are varied within predefined limits. Table 1 presents an overview of the parameters and their respective values used throughout this study unless stated otherwise. These values were selected to accurately represent the epidemiological dynamics of SARS-CoV-2.

6.1. Effect of the First Dose Vaccine

When a vaccine with 50% efficacy is introduced into a previously unvaccinated population, the number of exposed individuals decreases from 320 suspected cases to 302. However, with a more effective vaccine of 80% efficacy, the exposed population further declines to 284, as illustrated in Fig.2. Additionally, when the vaccination coverage rate rises from 10% to 50%, as shown in Fig. 3, the symptomatic population decreases from 120 to 62, with the peak delayed by nearly 50 days. If the vaccination coverage is further increased to 80%, the number of exposed individuals drops to 51. evident whenever infections occur. The numerical results demonstrate that higher vaccine efficacy and coverage significantly reduce the number of exposed and symptomatic cases while delaying the peak of infections, highlighting the potential impact of vaccination on controlling disease spread in public health policy.

6.2. Effect of the Second Dose Vaccine

Fig. 4 illustrates the impact of the second-dose vaccine efficacy on the dynamics of the exposed population using baseline values. Increasing the vaccine efficacy from 50% to 100% reduces the peak exposed population from 416 to 406. Furthermore, when the vaccination coverage rate rises from the baseline value of 8 individuals per 10,000 exposed to 800, and the vaccine efficacy increases from 50% to 100%, the exposed population declines from 256 to just 6 individuals, with the peak shifting from the 94th day to the 114th day, as depicted in Fig. 5.

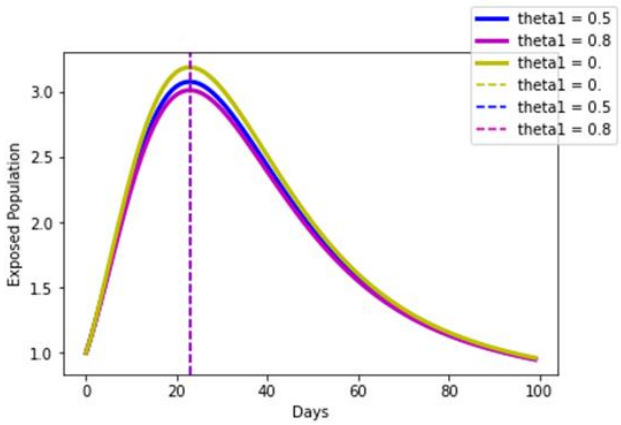

Fig. 2. Effect of Efficacy of the First Dose Vaccine

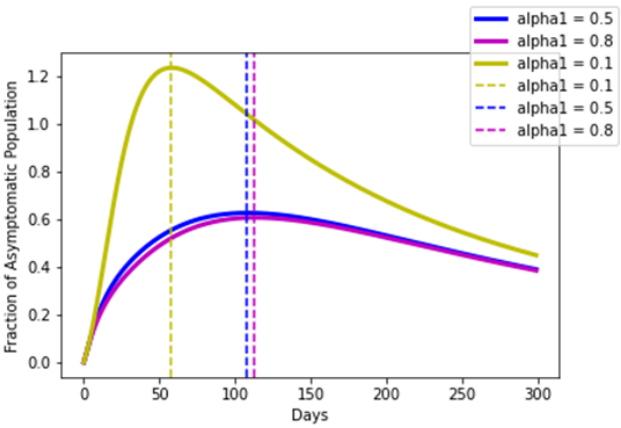

Fig. 3. Effect of Coverage Rate of the First Dose Vaccination

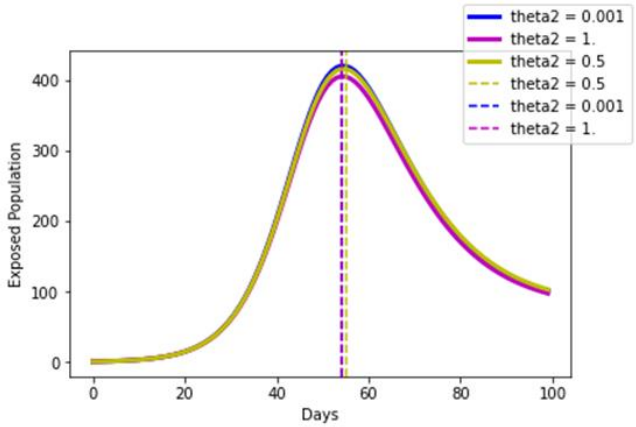

Fig. 4. Effect of Efficacy of the Second Dose Vaccine

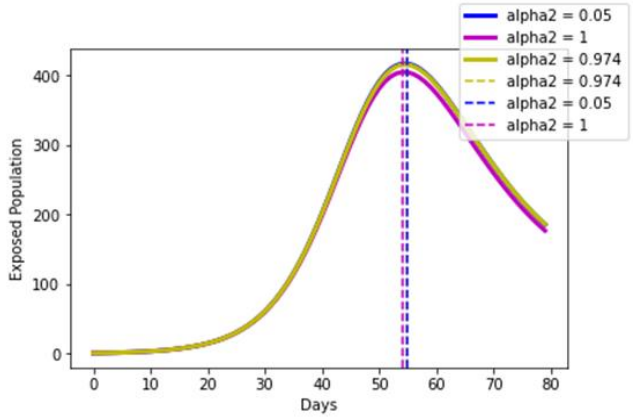

Fig. 5. Effect of Coverage Rate of the Second Dose Vaccination

6.3. Effect of the Use of Face - Mask

Fig. 6 illustrates the asymptomatic population over a 100-day period. It indicates that when face masks with 30% efficacy are used, the peak occurs on the 82nd day with 213 cases. This represents a slight reduction compared to the scenario without face masks, where 215 cases peak on the 79th day. If masks with approximately 50% efficacy are used, the peak shifts to the 85th day with 209 cases. Similarly, with 80% efficacy, the peak occurs on the 93rd day, reaching 197 cases.

Fig. 7 presents the asymptomatic population over the same period. It shows that increasing public compliance with face mask usage from 1% to 50% results in a marginal decrease in asymptomatic cases from 219 to 210. However, if compliance exceeds 80%, the asymptomatic population declines to 177 cases, with the peak shifting from the 64th day to the 86th day. The numerical results show that higher face mask efficacy delays the infection peak and reduces the asymptomatic population, emphasizing the role of mask-wearing in mitigating disease spread and informing public health policy.

6.4. Effect of the Quarantine

Fig. 8 illustrates the effect of varying the quarantine rate of exposed individuals on the asymptomatic population. Simulations indicate that increasing the quarantine rate by 20% reduces asymptomatic cases from 213 to 25 compared to the scenario without quarantine. When the quarantine rate is raised to 80% of exposed individuals, asymptomatic cases further decline to 8, while the peak shifts from the 213th day to the 187th day. However, achieving a higher quarantine rate requires extensive contact tracing and testing, which may be impractical for developing countries.

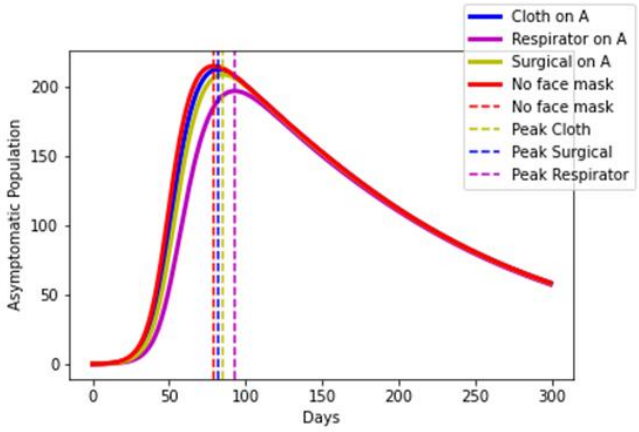

Fig. 6. Effect of type of Face Mask on Asymptomatic

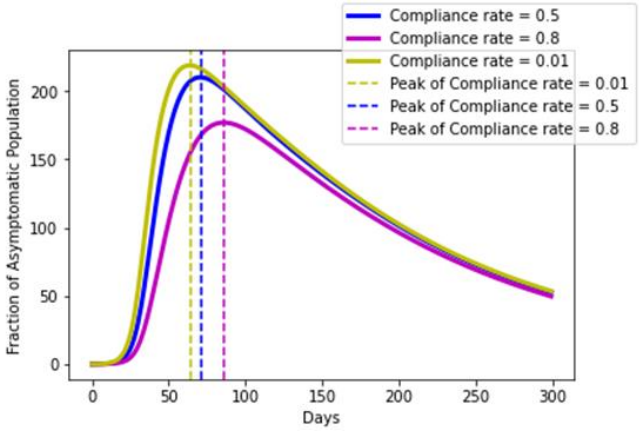

Fig. 7. Effect of consistent of use of Masks on Asymptomatic

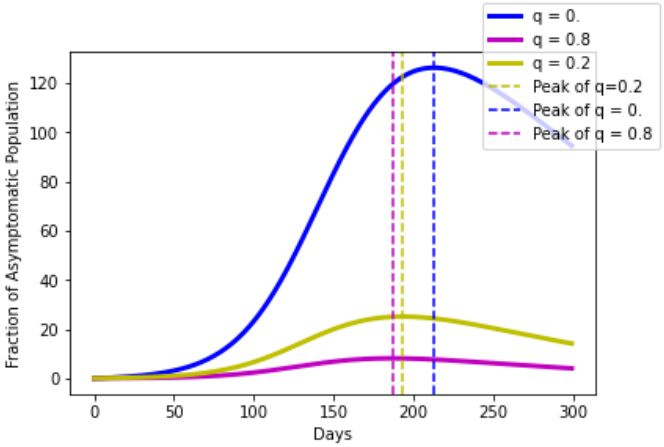

Fig. 8. Effect of quarantine rate on the Asymptomatic

7. Conclusion

This study employed a compartmental model to analyze COVID-19 transmission with vaccination. The vaccinated population was categorized into two groups: those who received only the first dose and those who completed both doses. Using the next-generation matrix approach, the basic reproduction number (R_0) under vaccination was determined. The model's disease-free and endemic equilibria were established, demonstrating that the disease-free equilibrium and endemic equilibrium are locally asymptotically stable when the control reproduction number $R_0 < 1$ and unstable when $R_0 > 1$. Overall, the success of a vaccination campaign depends on two key factors: vaccine efficacy and the proportion of the population vaccinated. When both factors are maximized, disease eradication becomes achievable. As a direction

for further study, incorporating stochasticity into the model would enhance its realism and better capture the inherent variability in real-world epidemics.

References

[1] H. M. Wanjala, M. O. Okongo, and J. O. Ochwach," Impact of Media Awareness and Use of Face-Masks on Infectious Respiratory Disease, *"Pan-American Journal of Mathematics*, 2, 15. 2023

[2] Organization, W. H. et al. (2020). Coronavirus disease 2019 (covid-19) situation report–1.

[3] R. M. Anderson, C. Fraser, A. C. Ghani, C. A. Donnelly, S. Riley, and N. M. Ferguson, "Epidemiology, transmission dynamics and control of SARS: the 2002–2003 epidemic," *Philosophical Transactions of the Royal Society of London. Series B: Biological Sciences*, vol. 359, no. 1447, pp. 1091–1105, 2004.

[4] S. P. Brand et al., "Forecasting the scale of the COVID-19 epidemic in Kenya," *MedRxiv*, 2020.

[5] S. Cauchemez et al., "Middle East respiratory syndrome coronavirus: quantification of the extent of the epidemic, surveillance biases, and transmissibility," *The Lancet Infectious Diseases*, vol. 14, no. 1, pp. 50–56, 2014.

[6] World Health Organization, "Coronavirus disease 2019 (COVID-19) situation report–156," 2023.

[7] H. A. Adekola, I. A. Adekunle, H. O. Egberongbe, S. A. Onitilo, and I. N. Abdullahi, "Mathematical modeling for infectious viral disease: The COVID-19 perspective," *Journal of Public Affairs*, vol. 20, no. 4, p. e2306, 2020.

[8] H. M. Wanjala, M. Okongo, and J. Ochwach," Mathematical Model of the Impact of Home-Based Care on Contagious Respiratory Illness Under Optimal Conditions." *Jambura Journal of Biomathematics (JJBM)*, 5(2), 83-94, 2024

[9] M. Kretzschmar and J. Wallinga, "Mathematical models in infectious disease epidemiology," in *Modern Infectious Disease Epidemiology*, pp. 209–221, 2009.

[10] S. Nagunuri and W. Tavernetti, "Mathematical modelling of epidemiology," *Journal of Student Research*, vol. 10, no. 3, 2021.

[11] K. Chaabna, S. Doraiswamy, R. Mamtani, and S. Cheema, "Facemask use in community settings to prevent respiratory infection transmission: A rapid review and meta-analysis," *International Journal of Infectious Diseases*, vol. 104, pp. 198–206, 2021.

[12] S. E. Eikenberry et al., "To mask or not to mask: Modeling the potential for face mask use by the general public to curtail the COVID-19 pandemic," *Infectious Disease Modelling*, vol. 5, pp. 293–308, 2020.

[13] F. M. Magpantay, "Epidemiological consequences of imperfect vaccines for immunizing infections," *SIAM Journal on Applied Mathematics*, vol. 74, no. 6, pp. 1810–1830, 2014.

[14] E. A. Iboi, O. O. Sharomi, C. N. Ngonghala, and A. B. Gumel, "Mathematical modeling and analysis of COVID-19 pandemic in Nigeria," *MedRxiv*, 2020.

[15] M. Loeb et al., "Effect of influenza vaccination of children on infection rates in Hutterite communities: a randomized trial," *JAMA*, vol. 303, no. 10, pp. 943–950, 2010.

[16] V. Bitsouni, N. Gialelis, and I. G. Stratis, "A model for the outbreak of COVID-19: Vaccine effectiveness in a case study of Italy," *arXiv*, 2020.

[17] P. Akuka, B. S., and C. Bornaa, "Mathematical Analysis of COVID-19 Transmission Dynamics Model in Ghana with Double-Dose Vaccination and Quarantine," *Computational and Mathematical Methods in Medicine*, 2022.

[18] S. Sharbayta, H. D. Desta, and T. Abdi, "Mathematical modelling of COVID-19 transmission dynamics with vaccination: A case study in Ethiopia," *medRxiv preprint*, 2023.

[19] S. Mwalili, M. Kimathi, V. Ojiambo, D. Gathungu, and R. Mbogo, "SEIR model for COVID-19 dynamics incorporating the environment and social distancing," *BMC Research Notes*, vol. 13, no. 1, pp. 1–5, 2020.

[20] V. N. Ojiambo, M. Kimathi, S. Mwalili, D. Gathungu, and R. Mbogo. "A human-pathogen seir-p model for covid-19 outbreak under different intervention scenarios in kenya." *medRxiv*, 2020.

[21] I. M. Wangari, S. Sewe, G. Kimathi, M. Wainaina, and W. Kaluki, "Mathematical Modelling of COVID-19 Transmission in Kenya: A Model with Reinfection Transmission Mechanism," *Computational and Mathematical Methods in Medicine*, 2020.

[22] Z. B. Dieudonne, "Mathematical model for the mitigation of the economic effects of the COVID-19 in the Demo-´cratic Republic of the Congo," *PLOS ONE*, 2021.

[23] I. Ahmed, G.U. Modu, A. Yusuf, P. Kumam, and I. Yusuf, "A mathematical model of coronavirus disease (covid-19) containing asymptomatic and symptomatic classes," *Results in Physics*, 21:103776, 2021.

[24] C. Castillo-Chavez, and B. Song, "Dynamical models of tuberculosis and their applications." *Mathematical Biosciences & Engineering, 1(2), 361-404, 2004*

[25] *H. M. Wanjala, "Mathematical Modelling of SARS-CoV-2 Incorporating Non-Pharmaceutical Interventions Coupled with Vaccination," Doctoral dissertation, Chuka University, 2023.*

[26] *G. Sepulveda, A. J. Arenas, and G. Gonzalez-Parra, "Mathematical Modeling of COVID-19 dynamics under two vaccination doses and delay effects,"* MDPI, *2023.*

Authors' Profiles

Henry M. Wanjala, PhD candidate of Applied Mathematics, Chuka University. Areas of scientific interest: Mathematical Epidemiology, Mathematical Phytopathology, Dynamical Systems.

Mark O. Okongo, Associate Professor of Applied Mathematics, Chuka University. Areas of scientific interest: Mathematical Epidemiology, Mathematical Phytopathology, Dynamical Systems.

Jimrise O. Ochwach, Lecturer of Applied Mathematics, Mama Ngina University College. Areas of scientific interest: Mathematical Epidemiology, Mathematical Phytopathology, Dynamical Systems.

How to cite this paper: Henry M. Wanjala, Mark O. Okongo, Jimrise O. Ochwach, "Mathematical Model of an Infectious Respiratory Disease with a Double-Dose Vaccine, Isolation and Use of Face-Mask", International Journal of Mathematical Sciences and Computing(IJMSC), Vol.11, No.2, pp. 10-27, 2025. DOI: 10.5815/ijmsc.2025.02.02